ISSN 0210-6558

Boletín de la Sociedad Española de Mineralogía

Una revista europea de Mineralogía, Petrología, Geoquímica y Yacimientos Minerales

Directora: P. Fenoll Hach-Alí

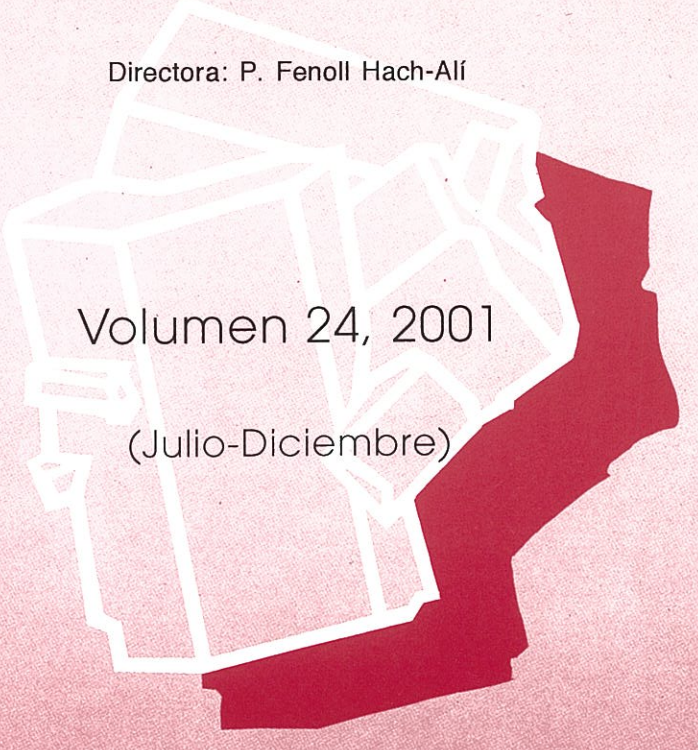

Volumen 24, 2001

(Julio-Diciembre)

Publicado por la Sociedad Española de Mineralogía con la colaboración del Ministerio de Educación y Cultura
Alenza, 1 - 28003 MADRID

Boletín de la Sociedad Española de Mineralogía

Vol. 24 Periodicidad semestral ISSN 0210-6558

Volumen 24, 2001
(Julio - Diciembre)

Publicado por la Sociedad Española de Mineralogía
(integrada en la "European Mineralogical Union")

Sociedad Española de Mineralogía
www.ehu.es/sem
Alenza, 1 - 28003 Madrid

BOLETÍN DE LA SOCIEDAD ESPAÑOLA DE MINERALOGÍA
Volumen 24 (2001)
(Julio-Diciembre)

ÍNDICE

Parte de los trabajos que se publican en éste volumen se han presentado como conferencias en la XXI Reunión de la Sociedad Española de Mineralogía y han sido supervisados por dos especialistas seleccionados de entre el grupo de revisores con que cuenta el Boletín de la Sociedad Española de Mineralogía y de acuerdo con el Comité de Redacción.

Depósito Legal: GR-491-1990 I.S.S.N.: 0210-6558

Imprime: Gráficas Fernando, Polígono Juncaril, Parc. 114-K, Albolote (GRANADA)

Mineralogical and geochemical characteristics of tin-bearing quartz veins, Ervedosa deposit, Northern Portugal

Características mineralógicas y geoquímicas de las venas de cuarzo-estanníferas del depósito de Ervedosa, Norte de Portugal

M. Elisa P. GOMES[1] and Ana M. R. NEIVA[2]

[1] Department of Geology, University of Trás-os-Montes and Alto Douro, Ap. 1013, 5001-911 Vila Real, Portugal (mgomes@utad.pt)
[2] Department of Earth Sciences, University of Coimbra, 3000-272 Coimbra, Portugal (neiva@ci.uc.pt)

Abstract: Tin-bearing quartz veins at the Ervedosa deposit intruded Silurian mica schists and quartzites and a 327 ± 9 Ma muscovite granite. They formed from hydrothermal fluids related to this highly-fractionated granite, which is the youngest of a granitic suite. The veins fill faults related to the Hercynian movements along a dextral N30°W shear zone and were exploited for cassiterite. The primary minerals from these veins belong to three paragenetic stages separated by faulting. Euhedral to subhedral crystals of cassiterite are generally <10 mm across, but they are locally associated in round masses with a diameter of 10 cm. The cassiterite shows alternating parallel darker and lighter zones. The darker zones are strongly pleochroic, oscillatory zoned and have more Fe, Nb + Ta and less Ti + Sn than the lighter zones, which are nearly pure SnO_2. The darker zones show exsolved columbite, titanian ixiolite, W ≥ Ti - ixiolite, niobian rutile and very rare wolframite. Arsenopyrite is the most abundant sulphide. Stannite occurs with quartz in veinlets cutting other sulphides and cassiterite and filling fractures in chalcopyrite.

Key words: tin-bearing quartz veins, Ervedosa deposit, muscovite granite, cassiterite, stannite, exsolutions.

Resumen: Las venas de cuarzo estanníferas del depósito de Ervedosa intruyen en micacitas y cuarcitas del Silúrico y en granito moscovítico de 327 ± 9 Ma. Las venas se formaron a partir de fluidos hidrotermales relacionados con el citado granito muy fraccionado, que es más joven de la serie granítica. Las venas rellenan fallas relacionadas con los movimentos hercínicos que se desarrollaron a lo largo de una zona de cisalla de dirección N30°W y fueron explotadas para casiterita. Los minerales primários de estas venas se desarrollan en tres etapas paragenéticas separadas por fallamiento. Los cristales euhédricos a subeuhédricos de casiterita son generalmente < 10 mm, y localmente se asocian dando agregados de 10 cm. La casiterita muestra bandas claras y oscuras paralelas alternantes. Las zonas oscuras son fuertemente pleocroicas, estan zonadas oscilatoriamente y tienen más Fe, Nb + Ta y menos Ti + Sn que las zonas claras, las cuales son SnO_2 casi puro. Las zonas oscuras muestran columbita, ixiolita titanifera, ixiolita W ≥ Ti, rutilo rico en niobio y muy poca wolframita. La arsenopirita es el sulfuro más abundante. La estannina, junto con cuarzo, se localiza en vetas que cortan a otros sulfuros y casiterita y rellena, además, algunas de las fracturas de la calcopirita.

Palabras clave: venas de cuarzo estanníferas, depósito de Ervedosa, granito moscovítico, casiterita, estannina, exsoluciones.

Introduction

The Hercynian Belt in Europe is an important metallogenic province for tin, tungsten, gold and uranium (Murciego *et al.*, 1997). The Cornwall tin province is the most important European tin producer and tin mineralizattion is related with highly evolved granites (Lehmann, 1990). There are many occurrences of tin and tungsten in Northern Portugal (Cotelo Neiva, 1944). Two types of mineralization are dominant: a. cassiterite in granitic pegmatites; b. cassiterite ± wolframite ± scheelite in quartz veins. Their genetic linkage with Hercynian granites is well accepted (Lécolle *et al.*, 1981; Neiva, 1984, 1987, 1993; Noronha *et al.*, 1987; Adam and Gagny, 1989; Gomes, 1996).

At Ervedosa, quartz veins contain cassiterite and rare stannite (Gomes, 1996). They are associated with a Hercynian tin-bearing muscovite granite which contains rare magmatic crystals of cassiterite. Close to this area, there are quartz veins with cassiterite and scheelite at Trigueiriça, Carvalhal, Agrochão and Murçós which are associated with Hercynian two-mica granites. These deposits occur in the vicinity of the Laza-Rebordelo ductile shear zone cutting either granitic rocks or the surrounding metamorphic rocks. This ductile shear zone corresponds to a complex lineament which continues to Spain, where there are similar mineralizations (Gomes, 1996). Therefore this study of the Ervedosa deposit is a contribution to help to understand a broad belt of Hercynian tin ores.

Prospect shafts were first developed when the Ervedosa deposit was identified in 1908 (Gomes, 1996). However, Freire D´Andrade (1920) suggested that a small part of the Ervedosa deposit may have been removed in ancient times by either Phoenicians or Romans. Between 1909 and 1927, the deposit was mined intermittently. From 1928 until 1969, the Ervedosa mine (also called Tuela mine) was worked by the Tuela Tin Mines Ldt. Company and produced about 6, 000 tonnes of tin and 6, 000 tonnes of As_2O_3 with 1.7 kg/m^3 of cassiterite (Casminex, unpub., company report, 1982). The exploitation started underground and continued upward into two large open pits; close to the end of development, alluvial placers were also exploited. They generally contained 1.8 kg/m^3 of cassiterite, but locally reached 4 kg/m^3. Lode mining ended when remaining cassiterite concentrations were ≤ 2 kg/tonne (Casminex, unpub., company report, 1982).

Geological Setting

The Ervedosa area is located in the Galiza-Trás-os-Montes Zone of the Iberian Terrane (Ribeiro *et al.*, 1990). This zone is composed by two domains separated by an important thrust (Farias Arquer, 1992): 1. The domain of mafic rock complex with five allocthonous massifs, which have been emplaced from the west over the Central Iberian Terrane (Ribeiro, 1974, Ribeiro *et al.*, 1990), and 2. The schistose domain of lower Silurian age, so-called "Peritransmontain Subdomain". At Ervedosa, this domain consists mainly of mica schists, phyllites and quartzites (Lécolle *et al.*, 1981), which are deformed by three tectonic deformation phases D1, D2 and D3 (Ribeiro, 1974).

At Ervedosa, a medium-grained slightly porphyritic muscovite-biotite granite, a medium- to fine-grained muscovite-biotite granite, and a fine- to medium-grained muscovite granite define a sequence of in situ fractional crystallization (Gomes, 1996). All of them are strongly peraluminous (A/CNK = 1.1-1.4) Hercynian granites. These three granites define a whole-rock Rb-Sr isochron which yields an age of 327 ± 9 Ma and an initial $^{87}Sr/^{86}Sr$ ratio of 0.7155 ± 0.0018 (Gomes and Neiva, 2002). They intruded the Silurian mica schists and the early Carboniferous medium- to coarse-grained

porphyritic biotite-muscovite granite (Fig. 1), but the contacts are sharp. The medium- to coarse-grained porphyritic muscovite-biotite granite surrounds the muscovite-biotite granites of the defined series and the contacts are sharp. The tin-bearing quartz veins intruded the Silurian mica schists, quartzites and muscovite granite (Fig. 1).

Cassiterite occurs rarely in centimeter-thick pegmatites. It is more common in N70°E-trending, dominantly subvertical quartz veins of < 0.2 m in thickness, and sometimes in N55°-70°S striking quartz veins which are 0.2 to 0.8 m thick, with lengths reaching a hundred meters. Stannite rarely occurs in these quartz veins and it is later than cassiterite, which is the main tin ore. Three hypogenic stages separated by Hercynian faulting were identified in these tin-bearing quartz veins (Gomes, 1996). A later stage characterized by supergenic phases and related to new fractures was also found.

Tin-bearing quartz veins are hosted in fractures which are related to the movements

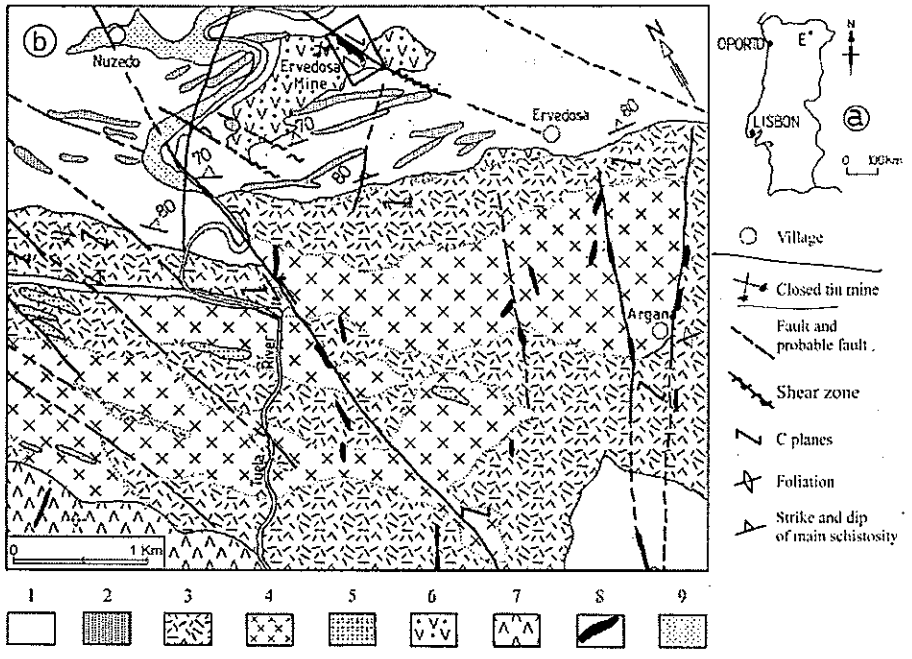

Fig. 1. a) Location of the Ervedosa area (E) on the map of Portugal; b) Geological map of Ervedosa area showing location of the Ervedosa deposit. The coordinates of Ervedosa mine are 7°05´70´´W, 41°43´40´´N. Lithounits: 1 - Silurian mica schists, 2 - Silurian quartzites, 3 - Early Carboniferous medium- to coarse-grained porphyritic biotite-muscovite granite, 4 - medium-grained slightly porphyritic muscovite-biotite granite, 5 - medium- to fine-grained muscovite-biotite granite, 6 - fine- to medium-grained muscovite granite, 7 - medium- to coarse-grained porphyritic muscovite-biotite granite, 8 - quartz veins, 9 - alluvial deposits.

Fig. 1. a) Localización del área de Ervedosa (E) en Portugal; b) Mapa geológico del área de Ervedosa con la localización del depósito de Ervedosa. Coordenadas de la mina de Ervedosa 7°05´70´´W, 41°43´40´´N. Litounidades: 1 - Micacitas del Silúrico 2 - cuarcitas del Silúrico, 3 - granito biotítico-moscovitico, de grano medio a groso, porfídico, del Carbonifero Inferior, 4 - granito moscovitico-biotítico de grano medio ligeiramente porfídico, 5 - granito moscovitico-biotítico de grano medio a fino, 6 - granito moscovitico de grano fino a medio, 7 - granito moscovitico-biotítico de grano medio a groso porfídico, 8 - venas de cuarzo, 9 - depósitos aluviales

along a dextral N30°W trending ductile shear zone, which is a component of the Laza-Rebordelo main shear zone (Fig. 2) (Gomes, 1996). These tin-bearing veins were probably derived from the late stages of fractional crystallization of the granite suite because magmatic fractionation was responsible for the increase in Sn contents of granites and their micas (Gomes and Neiva, 2002). In granites, Sn contents increase with magmatic

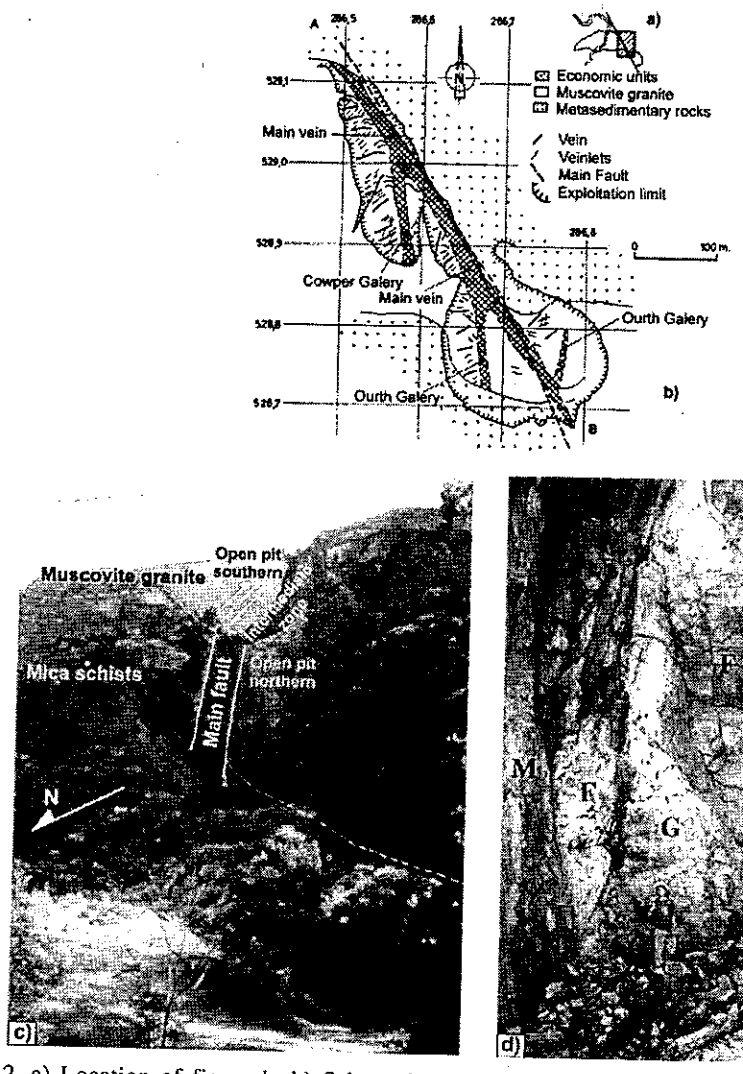

Fig. 2. a) Location of figura b. b) Schematic representation of Ervedosa quartz veins at the exploited superficial area (after Adam and Gagny, 1989); c) present aspect of two open pits; d) tin-bearing quartz veins highly deformed. Numbers 286,5 and 528,7 indicate kilometric coordinates, M - mica-schist, G - muscovite granite, F - quartz veins.

Fig. 2. a) Localización de la figura b. b) Representacion esquemática de las venas de cuarzo de Ervedosa explotada en superfície (segund Adam y Gagny, 1989); c) Aspecto actual de la exploración a cielo abierto; d) venas de cuarzo estannífero muy deformadas. Los números 286,5 y 528,7 indican coordenadas kilométricas, M - micacita, G - Granito moscovítico, F - Venas de cuarzo.

differentiation, which is mainly due to the increase in the amount of primary muscovite progressively richer in Sn. The highest tin enrichment was found in muscovite granite (68±18 ppm) and its muscovite, which is a tin-bearing granite. Therefore the tin-bearing quartz veins are probably genetically related to this muscovite granite.

Later barren quartz veins cut the tin-bearing veins. Very thin barren quartz veins, the so-called veinlets, cut the mineralized quartz veins and barren quartz veins.

Mineralogical characteristics and mineral paragenesis of the tin-bearing quartz veins

About fifty samples were collected from outcrops in the mine and from boreholes. Detailed studies of these samples included transmitted and reflected-light microscopy and electron-microprobe analyses. These studies were developed in order to establish the abundance, grain size, shape and contact relationships between the minerals and the paragenetic sequence (Tables 1 and 2).

Table 1. Mineralogy of tin-bearing quartz veins at the Ervedosa deposit, northern Portugal.
Tabla 1. Mineralogía de las venas de cuarzo estannífero del depósito de Ervedosa, Norte de Portugal.

MINERAL	ABUNDANCE	GRAIN SIZE	SHAPE	CONTACT RELATIONSHIPS
Rutile	rare	fine	acicular	included in quartz and exsolved from cassiterite.
Apatite	rare	fine	euhedral to subhedral	included in muscovite.
Muscovite	frequent	medium	subhedral, locally radial	2 generations: (1) intergrown with quartz and deformed; (2) radial, penetrated along fractures of cassiterite (Fig. 3a).
Quartz	abundant	fine to coarse	anhedral	in 3 stages: (1) earlier than sulphides; (2) and (3) in veins with sulphides and sulphosalts.
Fluorite	very rare	fine	anhedral	in veinlets with quartz.
Cassiterite	abundant	medium to coarse	subhedral to euhedral	penetrated by quartz and arsenopyrite (Fig. 3b).
Columbite-	very rare	fine	subhedral to euhedral	exsolved from cassiterite.
Ixiolite	very rare	fine	subhedral	exsolved from cassiterite (Fig. 3d).
Wolframite	very rare	fine	subhedral	exsolved from cassiterite.
Pyrrotite	rare	fine to medium	subhedral to anhedral	included in arsenopyrite (Fig. 4a) and pyrite.
Arsenopyrite	abundant	coarse to fine	euhedral to subhedral, later anhedral	2 generations: (1) associated with quartz and muscovite; (2) anhedral arsenopyrite, surrounded pyrite.
Bismuth	very rare	fine	subhedral	included in pyrite and in anhedral arsenopyrite (Fig. 4a).
Bismuthinite	rare	fine	subhedral to anhedral	included in anhedral arsenopyrite (Fig. 4b) and penetrating bismuth.
Matildite	very rare	very fine	subhedral	included in the latest anhedral arsenopyrite.
Pyrite	frequent	fine to coarse	subhedral to euhedral	surrounded, penetrated and replaced arsenopyrite.
Sphalerite	rare	fine to medium	anhedral	2 generations: (1) penetrated arsenopyrite and pyrite; (2) in bands with quartz.
Chalcopyrite	rare	medium to fine	subhedral to anhedral	2 generations: (1) exsolved from sphalerite as blebs (Fig. 4c); (2) with quartz and stannite in veinlets cutting arsenopyrite (Fig. 4d).
Stannite	rare	fine	anhedral	penetrated chalcopyrite; with quartz and chalcopyrite in veinlets cutting cassiterite.
Fe oxides	very rare	fine	anhedral	in veinlets cutting sulphides.
U oxides	very rare	fine	anhedral	in veinlets cutting sulphides.
Covellite	very rare	fine	anhedral	with quartz and chalcopyrite in veinlets cutting arsenopyrite.
Arsenates	very rare	fine to medium	anhedral	in veinlets cutting arsenopyrite.

Table 2. Mineral paragenesis of tin-bearing quartz veins from Ervedosa deposit.
Tabla 2. Paragenesis mineral de las venas de cuarzo estannífero del depósito de Ervedosa.

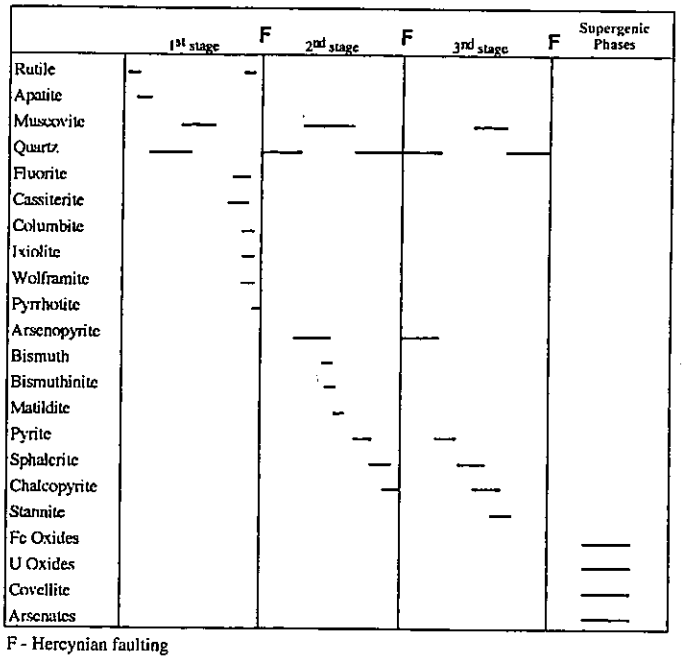

F - Hercynian faulting

Subhedral to euhedral cassiterite occurs in quartz veins. The cassiterite replaces quartz and muscovite in the veins. Crystals of cassiterite are generally less than 10 mm across and are locally cut by fractures filled with radial muscovite (Fig. 3a), quartz and arsenopyrite (Fig. 3b) or quartz, chalcopyrite and stannite. Crystals of cassiterite are also locally found in round masses with a diameter of less than 10 cm. Cassiterite exhibits narrow and parallel, alternating lighter and darker growth-zones (Fig. 3b). The lighter zones are translucent, colorless to tan, whereas the darker zones are strongly pleochroic (ε - red, ω - colorless) and oscillatory zoned (Fig. 3c). Exsolution products, commonly columbite and ixiolite (up to 20 x 15 μm) and rarely rutile (10 x 5 μm) and wolframite (5 x 5 μm), were mainly found in darker zones (Fig. 3d). They also, however, may occur in lighter zones close to the contact with darker zones. Cassiterite only belongs to the first stage of the mineralization (Table 2).

Stannite is rare, anhedral, fine-grained and penetrated chalcopyrite. It also occurs with quartz and chalcopyrite in veinlets cutting cassiterite and arsenopyrite. Stannite is the youngest sulphide mineral. It belongs to the third hypogenic stage (Table 2).

Non tin-minerals are silicates (quartz and muscovite), sulphides, sulphosalts and oxides. Arsenopyrite is the most abundant sulphide mineral. The main sulphide associations are presented in Fig. 4. The mineral paragenesis is given (Table 2) and shows three distinct hypogenic stages, each separated by Hercynian faulting. Some minerals reccur throughout the paragenesis. Quartz dominates in each stage. Supergene iron oxides, uranium oxides, covellite and arsenates were also observed in fine fractures formed after the last Hercynian faulting. These fractures cross all the sulphide minerals.

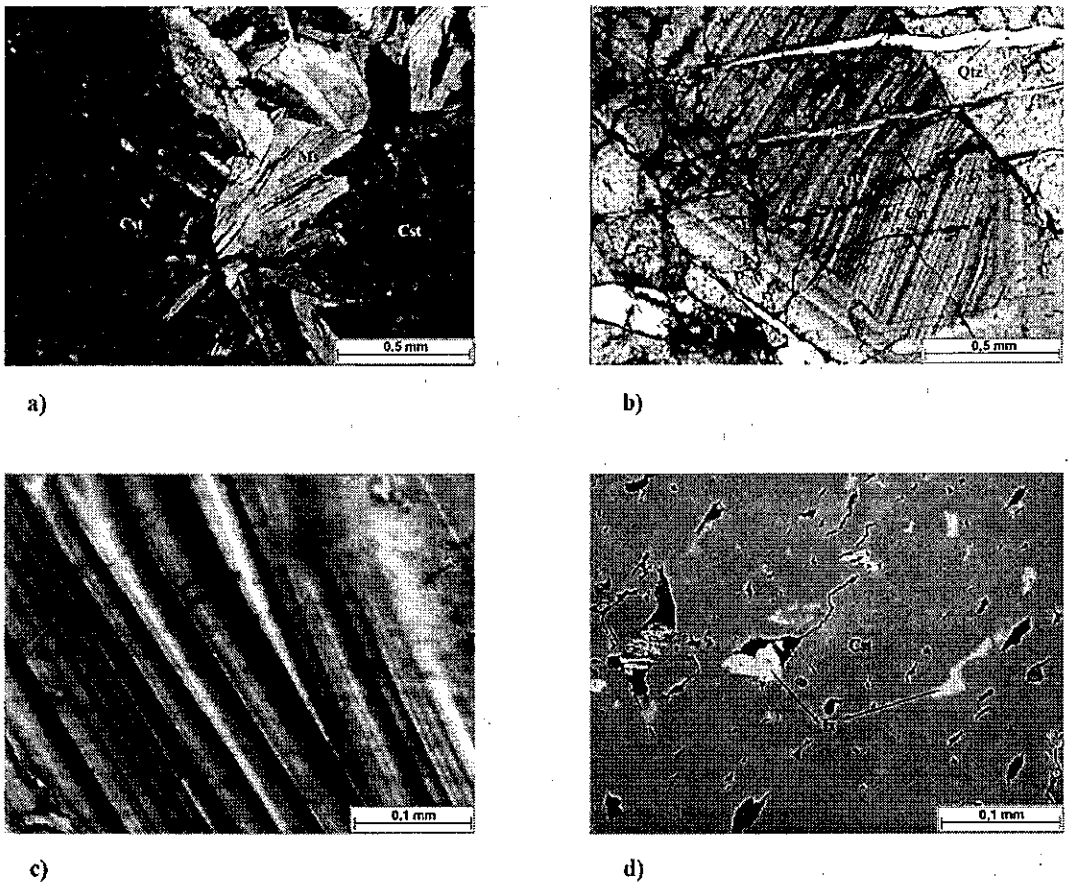

a) b)

c) d)

Fig. 3. a) Cassiterite (Cst) from the tin-bearing quartz veins with radial muscovite (Ms) penetrating along fractures; b) subhedral complexly zoned cassiterite cut by veinlets of quartz and arsenopyrite (Qzt); c) part of a crystal of cassiterite with the darker zones oscillatory zoned; d) cassiterite with ixiolite (Ix) exsolutions.

Fig. 3. a) Casiterita (Cst) de las venas de cuarzo estaníferas con moscovita radial (Ms) penetrando a lo largo de las fracturas; b) casiterita subhédrica con zonación compleja cortada por vetas de cuarzo y arsenopirita (Qzt); c) parte de un cristal de casiterita con zonas oscuras y zonación compleja; d) casiterita con exoluciones de ixiolita (Ix) .

Geochemical characteristics of minerals from the tin-bearing quartz veins

Analytical Methods

The electron microprobe analyses were performed to determine the mineral compositions, chemical zoning and to identify and analyse the exsolved minerals in cassiterite. The minerals were analysed on a Cameca Camebax electron microprobe at the Instituto Geológico e Mineiro, S. Mamede de Infesta, Portugal. Analyses were conducted at an accelarating voltage of 15 kV and a beam current of 20 nA for oxides and sulphides and 15 nA for muscovite. The trace elements of muscovite, separated with a magnetic separator and heavy liquids, from muscovite granite and tin-bearing quartz veins were determined by X-ray fluorescence (XRF) at Manchester University, U. K., with

precisions better than ± 1% for Rb and of ± 4% for the other trace elements. In muscovite concentrates, FeO was determined by titration with a standardized potasssium permanganate solution and Li was analysed by atomic absorption with precisions of ± 1 % and ± 2 % respectively.

Muscovite

In the tin-bearing quartz veins, the radial muscovite (generation 2) is richer in Si, Mg and F and poorer in Al than the subhedral muscovite intergrown with quartz (generation 1) (Tables 1 and 3), which is the most abundant. It was impossible to separate pure radial muscovite for the determinations of trace elements, because of its small grain-size and small amount.

The subhedral muscovite separated from the tin-bearing quartz veins is hydrothermal and richer in Sn and poorer in Fe, Nb, Zn, Rb and Cs than the primary muscovite from the

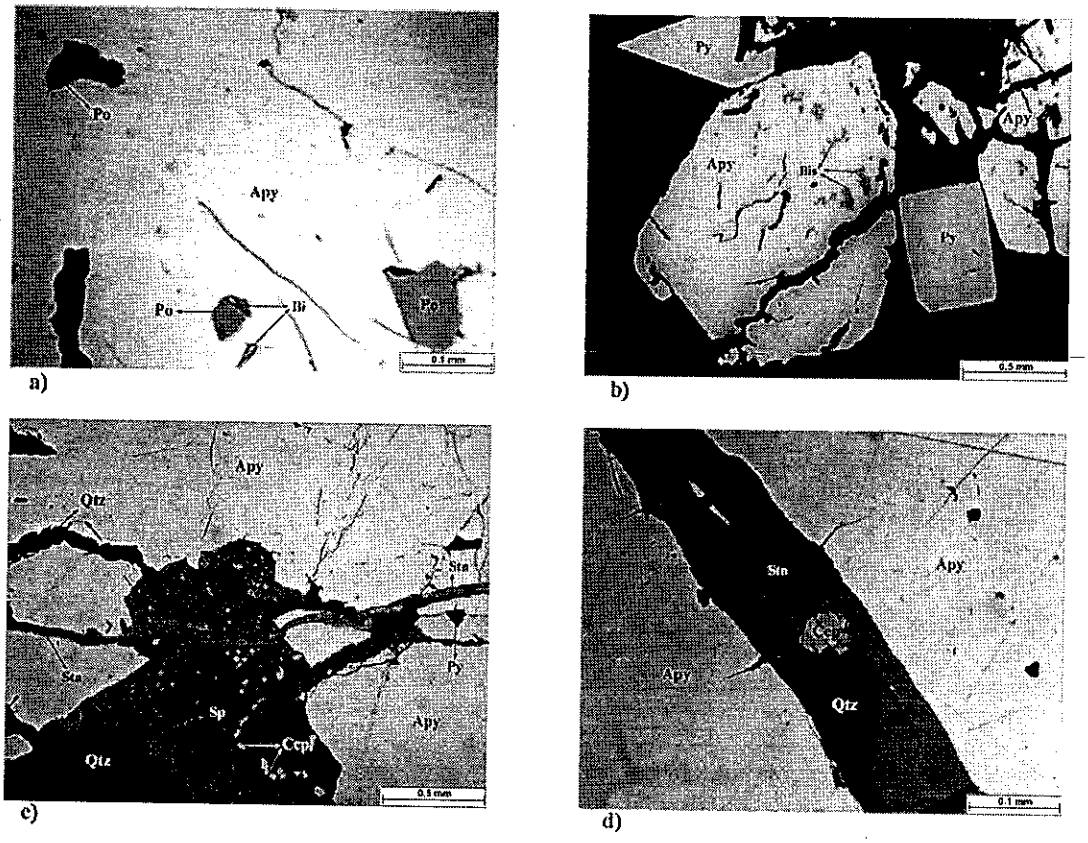

Fig.4. a) Arsenopyrite (Apy) with pyrrotite (Po) and bismuth (Bi) inclusions; b) Euhedral pyrite (Py) and arsenopyrite (Apy) with bismuthinite (Bis) inclusions; c) sphalerite (Sp) with exsolved chalcopyrite (Ccp) as blebs replacing quartz (Qzt) and veinlets of quartz, pyrite and stannite (Stn); d) stannite, chalcopyrite and quartz in veins cutting arsenopyrite.

Fig.4. a) Arsenopirita (Apy) con pirrotina (Po) e inclusiones de bismuto (Bi); b) Pirita idiomorfa (Py) y arsenopirita (Apy) con inclusiones de bismutinita (Bis); c) Esfalerita (Sp) con calcopirita exsuelta (Ccp) como gotas, substituyendo al cuarzo (Qzt) y vetas de cuarzo, pirita y estannina (Stn); d) estannina, calcopirita y cuarzo en venas cortando la arsenopirita.

Table 3. Average chemical analyses in wt. % and trace elements in ppm of muscovite from muscovite granite and tin-bearing quartz veins at Ervedosa deposit.
Tabla 3. Análisis químicos medios de elementos mayores (wt. %) y elementos traza (ppm) de moscovita del granito moscovítico y venas de cuarzo estannífero del depósito de Ervedosa.

	Magmatic Muscovite Muscovite granite		*Hydrothermal muscovite* Quartz veins subhedral		radial
	Mean	σ	Mean	σ	Mean
SiO_2	46.40	0.68	46.33	0.11	47.49
TiO_2	0.34	0.16	0.20	0.06	0.26
Al_2O_3	33.77	1.34	34.59	0.11	31.76
Fe_2O_3	0.92	0.64	0.74	0.23	n.a
FeO	2.58	0.55	1.33	0.32	2.01
MnO	0.04	0.06	0.12	0.02	0.14
MgO	0.62	0.32	0.42	0.07	1.76
Na_2O	0.47	0.17	0.33	0.03	0.26
K_2O	10.35	0.56	10.34	0.20	10.09
F	0.45	0.01	0.43	0.09	1.00
Cl	0.03		0.03	0.01	n.a
	95.97		94.86		94.77
O≡F	0.19		0.18		0.42
O≡Cl	0.01		0.01		-
Total	95.77		94.67		94.35
Cr	9	3	6	3	
V	20	9	21	13	
Nb	176	53	131	26	
Zn	215	66	126	31	
Sn	423	77	484	68	
Li	857	293	711	429	
Ni	55	17	7	3	
Zr	23	8	16	6	
Sc	8	1	*	*	
Y	111	62	81	10	
Sr	20	4	25	2	
Ba	66	22	88	35	
Rb	2269	409	1997	256	
Cs	85	26	34	6	
Ta	34	15	20	9	
Ce	29	15	36	24	
Nd	9	3	9	0	
La	30	5	22	5	
n	12		4		7

FeO of muscovite from granite and subhedral muscovite from quartz veins was determined in mica concentrates by a classical wet method. FeO of radial muscovite represents total FeO determined by electron-microprose; n.a. - not analysed; * - below the limit of sensitivity; n - number of analysed concentrates.
Analyst: M.E.P.Gomes.

muscovite granite (Table 3). Sn content of 484 ± 68 ppm of hydrothermal muscovite from tin-bearing quartz veins is close to the lowest Sn content (572 - 1503 ppm) of muscovite from other Portuguese tin-tungsten quartz veins (Neiva, 1982, 1987). The Sn content of 423 ± 77 ppm of magmatic muscovite from tin-bearing muscovite granite from Ervedosa is higher than those of 113 ± 31 ppm and 176 ± 59 ppm of muscovite from the muscovite-biotite granites of the defined granite suite from Ervedosa (Gomes, 1996) and higher than Sn content (144 - 210 ppm) of muscovite from other Portuguese tin-bearing granites (Neiva, 1975, 1987), but within the range (100 - 550 ppm) of Sn content of muscovite from tin-bearing aplites and pegmatites (Neiva, 1975, 1982). The modal amount of muscovite increases from 5.5 ± 1.7 in the oldest muscovite-biotite granite up to 13.5 ± 2.9 in the muscovite granite from the Ervedosa granite suite showing the increasing importance of muscovite in the Sn content of granites during fractional crystallization.

Cassiterite

The cassiterite crystals exhibit variable patterns (unzoned, oscillatory, simple and patchy zoning). Zoned crystals are the most common, with heterogeneous darker zones (Table 4). In general, the darker zones have higher Ta, Nb, Fe and Ti, and lower Sn contents than the lighter zones, which are nearly pure SnO_2 (Table 4 and Fig. 5b) as found by Neiva (1996) in cassiterite from other tin deposits.

Some single crystals are oscillatory zoned (Table 4). The pleochroism of darker zones can be mainly attributed to Nb, Fe and Ti (Neiva, 1996). The cassiterite structure allows the entrance of different cations as impurities in substitution for Sn^{4+} due to crystallochemical similarities (radius and electronegativity) in octahedral coordination. The alternance of darker and lighter zones is probably mainly controlled by the concentration and diffusion

Table 4. Representative electron-microprobe data on cassiterite from tin-bearing quartz veins at Ervedosa deposit.
Table 4. Datos de microsonda electrónica representativos de la casiterita de las venas de cuarzo estannífero del depósito de Ervedosa.

	Regularly zoned		Complexly oscillatory zoned					
	lighter	darker	core	1	2	3	4	rim
SnO_2	98.44	95.70	99.24	99.91	98.89	99.11	97.79	98.60
Nb_2O_5	0.54	1.60	0.55	0.29	0.73	0.47	0.51	0.73
Ta_2O_5	0.15	1.19	0.34	0.43	0.53	0.35	0.57	0.48
TiO_2	0.20	0.42	0.39	0.23	0.35	0.32	0.23	0.21
FeO	0.16	0.53	0.10	0.07	0.20	0.17	0.23	0.23
MnO	0.05	0.03	0.07	0.07	—	0.09	—	—
WO_3	—	0.02	—	—	0.11	—	0.01	0.36
Total	99.54	99.49	100.69	101.00	100.81	100.51	99.34	100.61
Sn	0.989	0.961	0.980	0.987	0.975	0.982	0.981	0.975
Nb	0.006	0.018	0.006	0.003	0.008	0.005	0.006	0.008
Ta	0.001	0.008	0.002	0.003	0.004	0.002	0.004	0.003
Ti	0.004	0.008	0.007	0.004	0.007	0.006	0.004	0.004
Fe	0.003	0.011	0.002	0.001	0.004	0.004	0.005	0.005
Mn	0.001	0.001	0.001	0.001	—	0.002	—	—
W	—	—	—	—	0.001	—	—	0.003
Ta/(Ta+Nb)	0.14	0.31	0.27	0.47	0.30	0.31	0.40	0.28

Oxides in wt. %, cation formula based on two atoms of oxygen.
Analyst: M.E.P.Gomes.

of elements and also by the growth dynamics of the crystals.

The cassiterite crystals analysed have more Fe than Mn and more Nb than Ta (Table 4), which is common in darker zones of cassiterite from pegmatites and quartz veins (Neiva, 1996; Murciego *et al.*, 1997). However the highest values found in cassiterite are 0.53 wt.% FeO, 1.60 wt.% Nb_2O_5, 1.19 wt. % Ta_2O_5 and 0.42 wt.% TiO_2. The analysed crystals show exsolved columbite, ixiolites, wolframite and rutile. The ratio (Ta+Nb)/(Fe+Mn) of cassiterite has values ranging between 0.6 and 12.0. The values less than 2 suggest that the Nb+Ta content in cassiterite is not exclusively controlled by the indistinguishable submicroscopic exsolved blebs of columbite and ixiolite. Similarly some of the Ti content of cassiterite may be attributed to exsolved rutile.

The (Nb, Ta) - (Fe, Mn) - (Sn, Ti,W) diagram (Fig. 5a) shows the triangular areas for cassiterite (Cst), rutile (Rt), columbite-

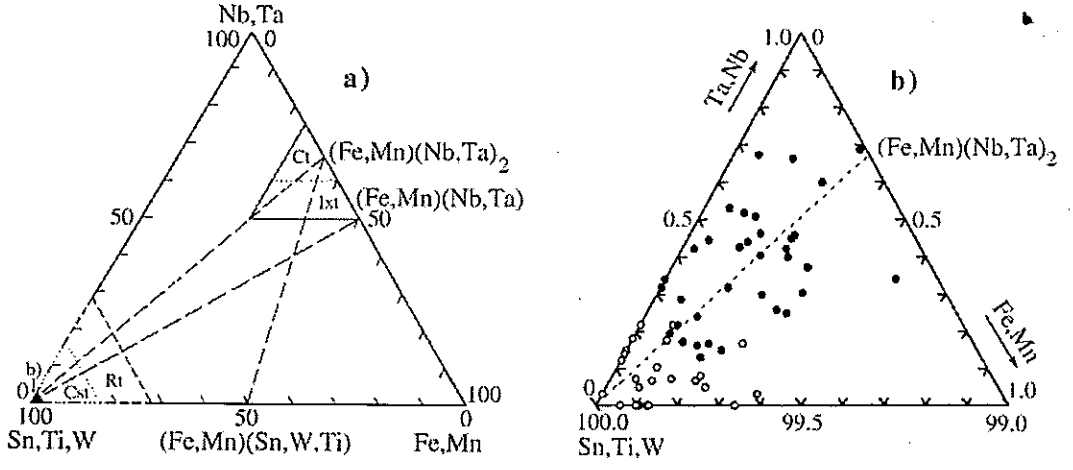

Fig. 5. a) (Nb,Ta) - (Fe,Mn) - (Sn,Ti,W) diagram showing the field boundaries of cassiterite (Cst), rutile (Rt), columbite-tantalite (Ct) and ixiolite (Ixt) from Neiva (1996) and the locations of the cassiterite, columbite-tantalite and ixiolite from Ervedosa; b) Compositions of cassiterite from quartz veins at Ervedosa. Symbols: ○- lighter zones and ●- darker zones of cassiterite.
Fig. 5. a) Diagrama (Nb,Ta) - (Fe,Mn) - (Sn,Ti,W) mostrando el limíte de los campos de casiterita (Cst), rutilo (Rt), columbita-tantalita (Ct) y ixiolita (Ixt) de Neiva (1996) y localización de casiterita, columbita-tantalita y ixiolita de Ervedosa; b) Composición de la casiterita de las venas de cuarzo de Ervedosa. Simbolos: ○- zonas claras y ●- zonas oscuras de casiterita.

tantalite (Ct) and ixiolite (Ixt). The compositions of cassiterite tend to fall close to the trend defined by the ideal substitution $(Fe,Mn)^{2+} + 2(Nb,Ta)^{5+} \rightleftarrows 3(Sn,Ti)^{4+}$ (Černý *et al.*, 1985). This substitution is restricted, but more effective in the darker zones than in the lighter zones of cassiterite.

Exsolved minerals in cassiterite

Compositions of products of exsolution from cassiterite, namely columbite, ixiolites, wolframite and rutile, are given in Table 5. Due to their small sizes, it was impossible to look for any zoning.

Exsolved minerals of ixiolite-wodginite family were distinguished from columbite-tantalite using the diagrams of Ta^{5+} versus Nb^{5+} and (Sn,Ti,W) - (Nb,Ta) - (Fe,Mn) (Figs. 6a, b), because it is impossible to get XRD data due to their small sizes. Recent data on ixiolite (Uher *et al.*, 1998) and wodginite (Tindle *et al.*, 1998; Galliski *et al.*, 1999) fall in their field in each of these diagrams. Some compositions from Ervedosa plot in the columbite-tantalite field between both boundaries, while those containing substantial contents of combined Ti, W and Sn fall below the lower boundary (Fig. 6a) and are arbitrarily called ixiolite. Ixiolite has lower levels of Nb+Ta and generally higher levels of Fe+Mn than columbite (Fig. 6b). Titanian ixiolite with subordinate Sn and W, but commonly with W>Sn has more Ti and less W than ixiolite with W≥Ti (Fig. 6c). Ixiolite has up to 12.38 wt. % WO_3.

Compositions of the exsolved orthorhombic phases range from ferrocolumbite to mangano-columbite (Fig. 6d). The ixiolite compositions have Ta/(Ta+Nb) and Mn/(Mn+Fe) similar to those of columbite, but they are not in contact. The niobian rutile does not contain Mn, so it plots along the Ta/(Ta+Nb) axis, while columbite and ixiolites cover most of the range of the Mn/(Mn+Fe)

Table 5. Compositions of products of exsolution in cassiterite from tin-bearing quartz veins at Ervedosa deposit.

Table 5. Composiciones de los productos de exolution de la casiterita das venas de cuarzo estannífero del depósito de Ervedosa.

	Columbite		Titanian ixiolite		Ixiolite with W≥ Ti		Wolframite	Rutile	
	Mean	σ	Mean	σ	Mean	σ	Mean	Mean	σ
Nb_2O_5	13.51	10.14	58.08	6.17	56.57	9.19	1.59	13.12	1.34
Ta_2O_5	63.02	10.16	12.69	7.50	12.88	8.21	0.24	5.81	2.07
TiO_2	2.69	0.40	4.01	1.02	2.23	0.26	0.06	72.06	2.98
SnO_2	1.01	0.16	1.47	1.10	0.57	0.32	0.31	1.71	0.17
WO_3	2.00	1.66	4.62	2.36	9.35	1.96	72.31	1.17	0.20
MnO	4.54	5.25	5.99	3.42	11.85	1.91	10.60	0.02	0.02
FeO	13.71	5.53	12.67	3.42	6.86	1.65	13.41	5.75	0.51
Total	100.48		99.53		100.31		98.52	99.64	
Nb	1.665	0.187	2.081	0.166	2.045	0.244	0.037	0.088	0.010
Ta	0.224	0.178	0.278	0.174	0.289	0.192	0.003	0.024	0.009
Ti	0.119	0.019	0.240	0.063	0.135	0.017	0.002	0.807	0.028
Sn	0.024	0.005	0.047	0.035	0.019	0.011	0.006	0.010	0.002
W	0.030	0.025	0.095	0.049	0.196	0.046	0.952	0.005	0.001
Mn	0.224	0.253	0.403	0.233	0.804	0.106	0.456		0.001
Fe	0.677	0.271	0.841	0.225	0.466	0.130	0.570	0.072	0.009
Total	2.963		3.985		3.954		2.026	1.006	
n	10		26		11		2	5	

Oxides in wt. %, n- number of analyses, cation formula based on the following atoms of oxygen; 6 for columbite, 8 for ixiolites, 4 for wolframite and 2 for rutile. Analyst: M. E.P. Gomes.

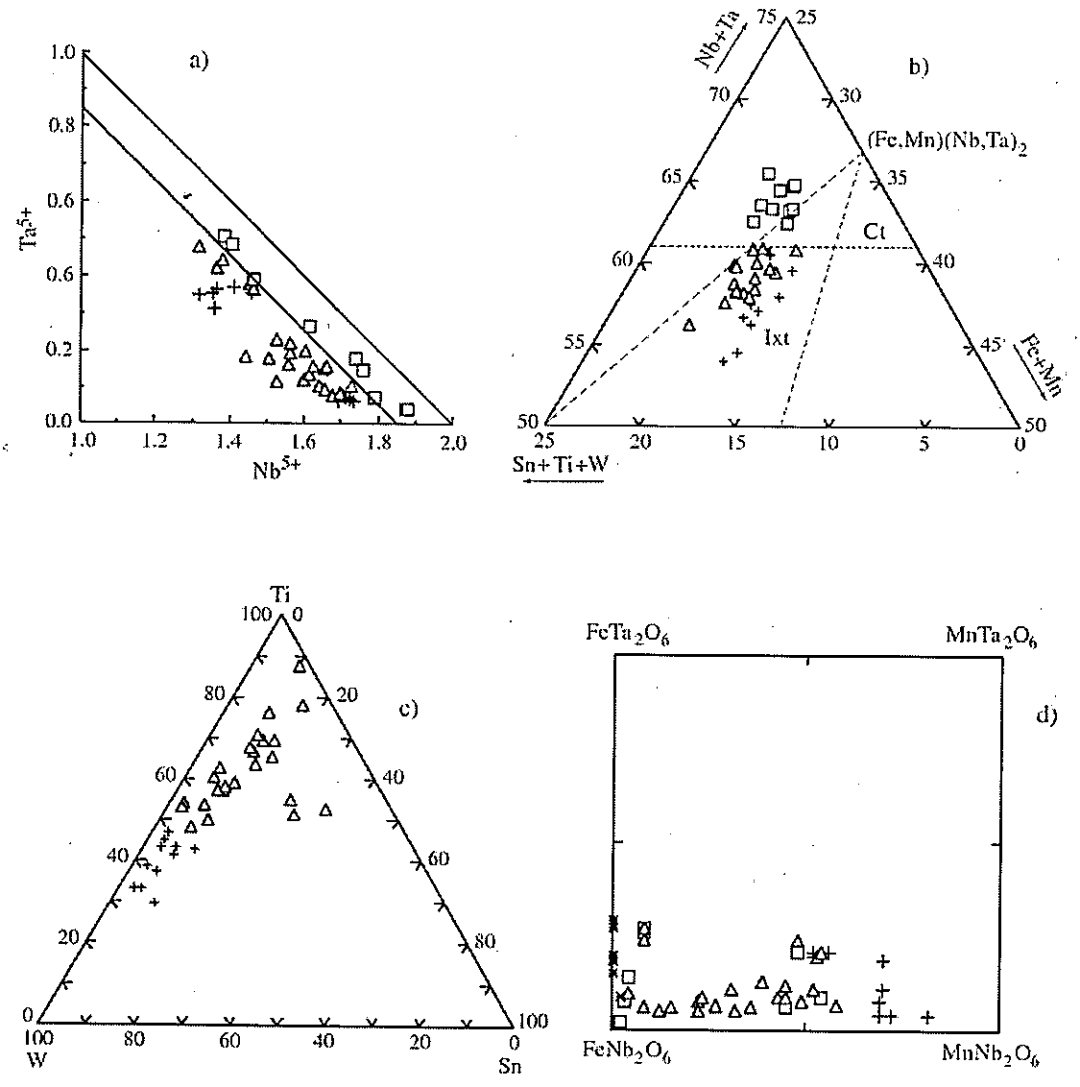

Fig. 6. a) Compositions of exsolved columbite and ixiolites from Ervedosa cassiterite. a. Diagram of Nb^{5+} versus Ta^{5+} with boundaries of Neiva (1996); b. (Sn,Ti,W) - (Nb, Ta) - (Fe, Mn) diagram, an enlargement of the triangular area Ct-Ixt shown in Fig. 5a, with the boundary between columbite-tantalite and ixiolite of Neiva (1996); c. Ti-Sn-W diagram; d. columbite quadrilateral which also includes the plots of niobian rutile. Symbols: □- columbite, △- titanian ixiolite commonly with W>Sn, + - ixiolite with W≥ Ti, ✻ - niobian rutile.

Fig. 6. a) Composición de las columbitas e ixiolitas exsueltas de la casiterita de Ervedosa. a. Diagrama de Nb^{5+} versus Ta^{5+} con los limítes de Neiva (1996); b. Diagrama (Sn,Ti,W) - (Nb, Ta) - (Fe, Mn), ampliación de la área triangular Ct-Ixt mostrada en la Fig. 5a, con el limíte entre columbita-tantalita y ixiolita de Neiva (1996); c. diagrama Ti-Sn-W; d. cuadrilátero de la columbita que incluye las proyecciones de rutilo rico en niobio. Simbolos: □- columbita, △- ixiolita titanifera geralmente con W>Sn, + - ixiolita con W≥ Ti, ✻ - rutilo rico en niobio.

values. The dominance of divalent cations facilitates exsolution of columbite and titanian ixiolite, whereas trivalent cations will lead to exsolution of titanian $(Fe,Sc)^{3+}NbO_4$ phases (Černý *et al.*, 1999).

In the (Sn,Ti,W) - (Nb,Ta) - (Fe,Mn) diagram (Fig. 7), the data on columbite plot above the (Sn,Ti,W) - $(Fe,Mn)(Nb,Ta)_2$ join, indicating a surplus of (Nb,Ta) over the stoichiometry of columbite. The ixiolites fall in their field. The titanian ixiolite with subordinate Sn and W show some alignment along the (Sn,Ti) - $(Fe,Mn)(Nb,Ta)_2$ join extending to columbite, suggesting that the substitution $(Fe,Mn)^{2+} + 2(Nb,Ta)^{5+} \rightleftarrows 3(Sn,Ti)^{4+}$ dominates

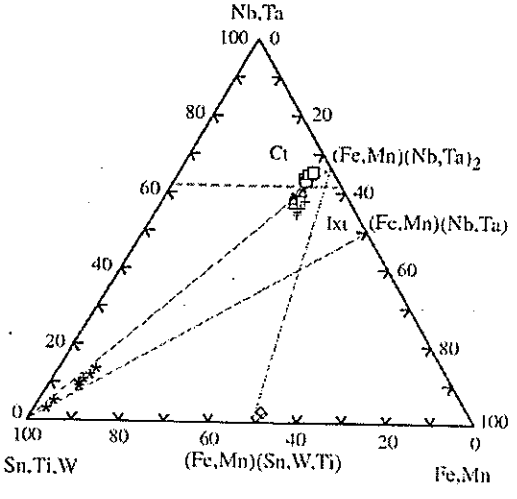

Fig. 7. Compositions of exsolved columbite, ixiolites, wolframite and rutile from Ervedosa cassiterite in the (Sn,Ti,W) - (Nb,Ta) - (Fe,Mn) diagram. For columbite and ixiolites only selected representative compositions were plotted. Symbols as in Fig. 6 and ◇-wolframite. Ct - columbite-tantalite, Ixt - ixiolite.

Fig. 7. Composiciones de columbita, ixiolitas, wolframita y rutilo exsueltas de la cassiterita de Ervedosa en el diagrama (Sn,Ti,W) - (Nb,Ta) - (Fe,Mn). Para las columbitas y ixiolitas solamente se han representado las composiciones más representativas. Símbología idéntica a la de Fig. 6 y ◇-wolframite. Ct - columbita-tantalita, Ixt - ixiolita.

(Černý *et al.*, 1986). The incorporation of W in ixiolite is explained by the substitution $W^{6+}(Ti,Sn)(Nb,Ta)^{5+}_2$ (Johan and Johan, 1994). The ixiolite with W≥Ti plots between the (Sn,Ti) - $(Fe,Mn)(Nb,Ta)_2$ and $(Fe,Mn)(Nb,Ta)_2$ - (Fe,Mn)(Sn,Ti,W) joins and below the data for columbite. So the increase in W content of ixiolite seems to be responsible for the shift towards the latter join and certainly drifting towards wolframite composition which was found as an exsolution product of cassiterite.

The exsolved wolframite plots, as expected, in the intersection of $(Fe,Mn)(Nb,Ta)_2$ - (Fe,Mn)(Sn, Ti,W) join with (Sn,Ti,W) - (Fe,Mn) join (Fig. 7). It has a higher ferberite content than heubnerite content (Table 5) and more Nb than Ta. The cation total normalized to four atoms of oxygen exceeds the ideal value of 2.00. Therefore, probably it contains some Fe^{3+}. The substitution $[Fe^{3+},(Nb,Ta)^{5+}] \rightleftarrows (Fe^{2+},W^{6+})$ modified from that of Polya (1988), explains the incorporation of Nb and Ta in wolframite. The incorporation of some Sn and Ti in wolframite (Table 5) may be explained by the substitution $2(Sn,Ti)^{4+} \rightleftarrows [(Fe,Mn)^{2+}, W^{6+}]$.

Rutile exsolutions are rare and contain Nb>Ta and Sn>W. So they are of niobian rutile (Černý *et al.*, 1999). The cation total normalized to two atoms of oxygen only exceeds slightly the ideal value of 1.00 (Table 5). Therefore it probably has a very low Fe^{3+} content, which is supported by the plot of rutile compositions between the (Sn,Ti,W) - (Fe, Mn)(Nb,Ta)$_2$ and (Sn,Ti,W) - (Fe,Mn)(Nb,Ta) joins (Fig. 7). The substitution $2(Nb,Ta)^{5+} + Fe^{2+} \rightleftarrows 3Ti^{4+}$ dominates and is responsible for the incorporation of Nb, Ta and Fe^{2+} in rutile. The substitution $Sn^{4+} \rightleftarrows Ti^{4+}$ explains the incorporation of Sn, while the substitution $W^{6+}Fe^{2+} \rightleftarrows 2Ti^{4+}$ may explain the incorporation of W and Fe in rutile.

Given suitable P-T conditions and probably the movement of late fluids, the cassiterite structure exsolves Nb, Ta, Fe, Mn, Ti and W, which form exsolved ferrocolumbite-manganocolumbite, ixiolites, wolframite and

rutile. Cassiterite from Portuguese tin and tungsten deposits commonly shows these products of exsolution, except wolframite (Neiva, 1996). No other reference of exsolved wolframite from cassiterite is known.

Sulphides and sulphosalts

Sulphide minerals were studied from the muscovite granite and from the tin-bearing quartz veins (Table 6). Stannite $(Cu_{1.94}Fe_{0.97}Zn_{0.09}Sn_{1.00}S_4)_{\Sigma 4}$ is the only tin sulphide mineral found in the tin-bearing quartz veins from Ervedosa, but it is rare and the last sulphide mineral.

Monoclinic pyrrhotite with the composition $Fe_{0.89}S_{1.00}$ was found in the muscovite granite and tin-bearing quartz veins. Arsenopyrite from muscovie granite and quartz veins has a composition of FeAsS. However arsenopyrite from muscovite granite is relatively the poorest in Fe and tends to be one of the richest in S (Figs. 8a, b). In the veins, the latest anhedral arsenopyrite has generally relatively higher Fe content than the earliest euhedral to subhedral arsenopyrite. Bismuthinite and matildite were only rarely found as small (8 x 5 μm) inclusions in the latest anhedral arsenopyrite and average compositions are given in Table 6. Matildite contains some additional Fe and Pb replacing Ag (e.g., Gaspar, *et al.*, 1987). The compositions of pyrite from muscovite granite and tin-bearing quartz veins are similar (Table 6). Pyrrhotite, arsenopyrite and pyrite are not

Table 6. Average electron-microprobe analyses (wt. %) of some sulphides and sulphosalts from muscovite granite and tin-bearing quartz veins at Ervedosa deposit.
Table 6. Análisis químicos medios (wt. %) de microsonda electrónica de algunos sulfuros y sulfosales del granito moscovítico e de las venas de cuarzo estannífero del depósito de Ervedosa.

		Cu	Ag	Au	Zn	Fe	Mn	Cd	Sb	As	Bi	Pb	Sn	S	Total	n
Pyrrhotite	G	0.03	n.d.	n.d.	0.03	59.16	n.d.	n.d.	n.d.	0.04	n.d.	0.18	n.d.	39.65	99.09	5
	Qz *st.1*	0.15	n.d.	n.d.	0.05	60.17	0.02	n.d.	n.d.	0.12	n.d.	n.d.	n.d.	39.16	99.67	11
Arsenopyrite	G	n.d.	n.d.	0.02	n.d.	33.78	n.d.	n.d.	n.d.	45.69	n.d.	n.d.	n.d.	19.96	99.45	4
	Qz *st.2*	n.d.	n.d.	n.d.	0.07	34.81	0.01	n.d.	n.d.	46.19	n.d.	n.d.	0.08	19.05	100.21	19
	Qz *st.3*	0.08	0.10	n.d.	0.07	35.60	0.04	n.d.	0.07	45.31	n.d.	n.d.	0.04	19.48	100.79	22
Bismuthinite	Qz *st.2*	0.38	0.25	n.d.	0.06	0.15	n.d	n.d.	n.d.	n.d.	78.07	0.87	0.08	19.13	98.99	5
Matildite	Qz *st.2*	n.d.	24.78	n.d.	0.13	1.75	n.d.	n.d.	n.d.	n.d.	55.41	2.15	n.d.	16.76	100.98	2
Pyrite	G	0.02	0.05	n.d.	0.09	45.85	0.06	n.d.	0.03	0.12	n.d.	n.d.	0.06	53.24	99.52	10
	Qz *st.2,3*	0	0.06	n.d.	0.10	46.50	0.03	n.d.	0.04	0.27	n.d.	n.d.	0.05	52.74	99.79	21
Sphalerite	G	0.13	0.02	n.d.	56.28	8.96	0.07	0.68	0.02	0.07	n.d.	n.d.	n.d.	33.82	100.05	17
	Qz *st.2*	0.05	n.d.	n.d.	59.92	6.41	0.12	0.63	n.d.	0.05	n.d.	n.d.	n.d.	33.47	100.65	4
	Qz *st.3*	0.24	0.30	n.d.	60.12	2.42	0.06	0.65	n.d.	0.01	n.d.	n.d.	n.d.	35.53	99.33	2
Chalcopyrite	G	35.72	n.d.	n.d.	0.04	28.42	n.d.	n.d.	n.d.	n.d.	n.d.	n.d.	n.d.	34.88	99.06	5
	Qz *st.2*	33.49	0.08	n.d.	1.79	28.98	0.03	n.d.	n.d.	0.04	n.d.	0.08	n.d.	34.92	99.41	13
	Qz *st.3*	33.46	0.02	n.d.	0.09	30.08	0.02	0.01	0.01	0.07	n.d.	n.d.	n.d.	35.02	98.78	12
Stannite	Qz *st.3*	28.41	0.18	0.02	1.36	12.51	0.03	0.09	n.d.	0.06	n.d.	n.d.	27.42	29.74	99.82	14

n - number of grains ; G - granite; Qz - quartz veins; *st. 1, 2, 3* - stages 1, 2, 3 from the paragenesis; n.d. - not detected
Analyst: M.E.P.Gomes.

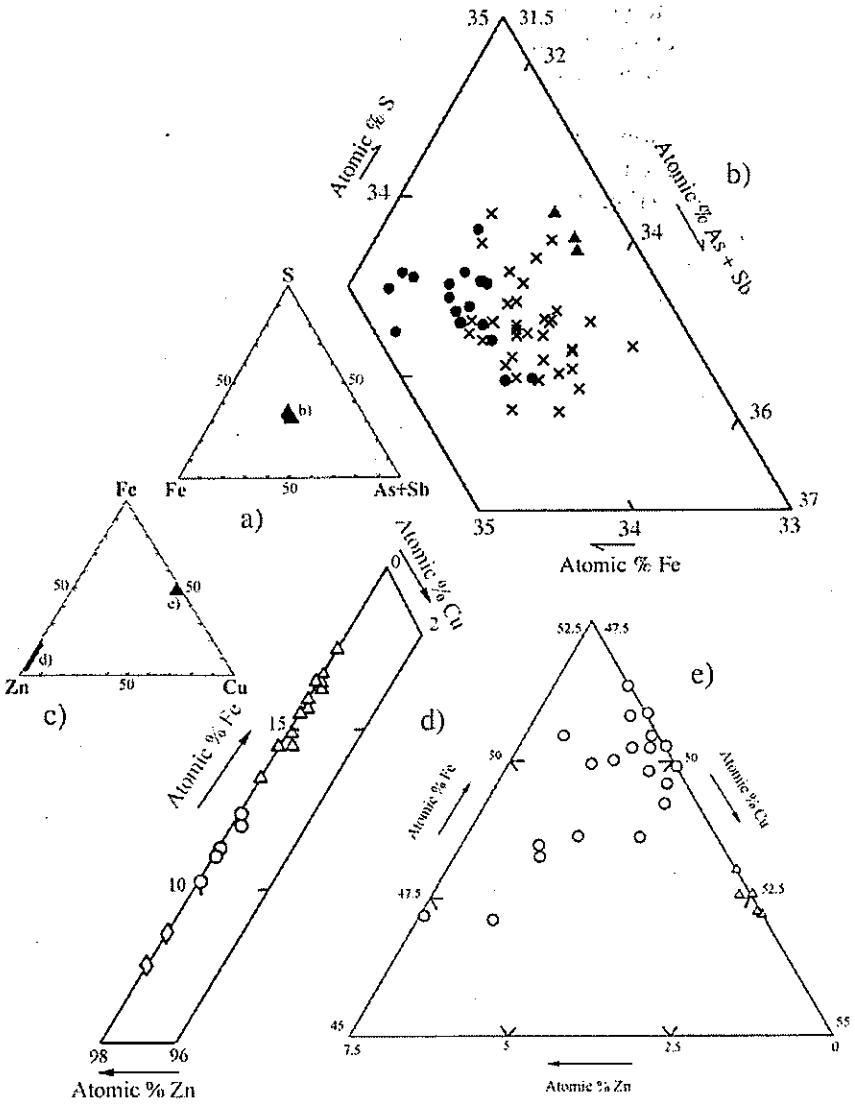

Fig. 8. Compositions of some sulphides from muscovite granite and tin-bearing quartz veins at Ervedosa. a) and b) compositions of arsenopyrite in the S-Fe-(As+Sb) diagram, with a) showing the location of diagram b). c) Zn-Fe-Cu diagram showing positions of diagrams d) and e). d) Compositions of sphalerites; e) compositions of chalcopyrite. Symbols: arsenopyrite from: ▲- muscovite granite; X- euhedral to subhedral, ● - anhedral from tin-bearing quartz veins. Sphalerite and chalcopyrite from: △- muscovite granite, ○- tin-bearing quartz veins,◇- the latest sphalerite from these veins.

Fig. 8. Composiciones de algunos sulfuros del granito moscovitico y venas de cuarzo estannífero de Ervedosa. a) y b) composiciones de arsenopirita en el diagrama S-Fe-(As+Sb), indicando en a) la posición del diagrama b). c) diagrama Zn-Fe-Cu indicando las posiciones de los diagramas d) y e). d) Composiciones de esfaleritas; e) composiciones de calcopirita. Simbolos: arsenopirita de: ▲- granito moscovitico; X- euhédrica a subhédrica, ● - anhédrica de las venas de cuarzo estanníferas. Esfalerita y calcopirita de: △- granito moscovitico, ○- venas de cuarzo estannífero,◇- esfalerita tardia de esas venas.

in equilibrium in muscovite granite and tin-bearing quartz veins. Therefore crystallization temperatures cannot be estimated (Kretschmar and Scott, 1976).

Sphalerite from tin-bearing quartz veins is poorer in Fe and richer in Zn than sphalerite from muscovite granite (Fig. 8c, d). Fe substitutes for Zn. In these veins, later sphalerite in bands with quartz is poorer in Fe than the earlier sphalerite penetrating arsenopyrite and pyrite. Generally each sphalerite grain has an homogeneous composition, but locally in the tin-bearing quartz veins a small increase in FeS was found from rim to core in individual sphalerite crystals. The maximum variation in FeS mole % found in sphalerite grains is 13 - 17 in muscovite granite and 8 - 11 in tin-bearing quartz veins. These ranges may reflect variations in the activity of FeS in the fluid and in physico-chemical conditions during precipitation. Chalcopyrite from tin-bearing quartz veins is poorer in Cu and commonly richer in Zn and Fe than chalcopyrite from muscovite granite (Fig. 8c, e).

At Ervedosa the distinctions found in the chemical compositions of arsenopyrite, sphalerite and chalcopyrite from muscovite granite and tin-bearing quartz veins certainly reflect differences in compositions and temperatures of fluids. The hydrothermal fluids will be richer in Fe and Zn and of lower temperature than the fluids associated to the late stage of granite fractional crystallization.

Conclusions

1) The tin-bearing quartz veins at Ervedosa are related to hydrothermal fluids which circulated mainly through a system of Hercynian fractures in Silurian mica schists and quartzite and the Hercynian Sn-bearing muscovite granite along a dextral N30°W shear zone.

2) The mineral paragenesis shows three hypogenic stages.

3) Euhedral to subhedral cassiterite shows sequences of alternating parallel darker and lighter zones. The darker zones are strongly pleochroic, oscillatory zoned, richer in Fe, Nb, Ta, Ti and poorer in Sn than the lighter zones, which are nearly pure SnO_2.

4) The darker zones of cassiterite show exsolution blebs ranging from ferrocolumbite to manganocolumbite, also of ixiolites, rutile and very rarely of wolframite. Titanian ixiolite with subordinate W>Sn is richer in Ti and poorer in W than ixiolite with W≥Ti. Both ixiolites are richer in Fe+Mn and poorer in Nb+Ta than columbite. Rutile exsolutions have Nb>Ta, Sn>W and Fe. Wolframite exsolution with Fe > Mn has Nb > Ta.

5) Cassiterite is the main tin ore. Tin is also retained in hydrothermal muscovite, which is earlier or contemporaneous of cassiterite in quartz veins. It is richer in Sn and poorer in Fe, Nb, Zn, Rb and Cs than magmatic muscovite from the muscovite granite.

6) Arsenopyrite is the most abundant sulphide. Stannite is very rare and the last sulphide mineral, which cuts cassiterite.

7) The tin-bearing quartz veins at Ervedosa probably originated from hydrothermal fluids related to the Hercynian Sn-bearing muscovite granite, which is the youngest of a fractional crystallization suite.

Acknowledgements

Thanks are due to Prof. M. R. Machado Leite, Dr. J. M. F. Ramos and Mr. F. A. P. Santos for providing access to electron microprobe facilities at the Instituto Geológico e Mineiro, S. Mamede de Infesta, Portugal. We are grateful to Dr. J. Esson for electron microprobe and XRF facilities at the Department of Earth Sciences, University of Manchester, U. K.. This paper benefited from

the critical review of Prof. J. M. Cotelo Neiva and of an anonymous reviewer. Funding was provided by a grant of INIC, Portugal to M. E. P. Gomes. This research was carried out in the programme of Geosciences Centre, Coimbra University, Portugal.

References

Adam, D. and Gagny, C. (1989) Contrôle strutural et magmatique de la formation de gisements d'étain-tungstène du Tras-os-Montes Oriental (Portugal). Guides pour l'exploration miniére. *Chron. Rech. Min.* **496**, 57-74.

Casminex- prospecções mineiras, Lda: Unpublished technical report (1982), 9 pp.

Černý, P., Chapman, R., Simmons, W. B., Chackowsky, L. E. (1999) Niobian rutile from the McGuire granitic pegmatite, Park County, Colorado:Solid solution, exsolution, and oxidation. *Amer. Mineral.* **84**, 754-763.

Černý, P., Goad, B. E., Hawthorne, F. C. and Chapman, R. (1986) Fractionation trends of the Nb- and Ta- bearing oxide minerals in the Greer lake pegmatitic granite and its pegmatite aureole, Southeastern Manitoba. *Amer. Mineral.* **71**, 501-517.

Černý, P., Roberts, W. L., Ercit, T. S., and Chapman, R. (1985) Wodginite and associated oxide minerals from the Peerless pegmatite, Pennington Country, South Dakota. *Amer. Mineral.* **70**, 1044-1049.

Cotelo Neiva, J.M. (1944) - Jazigos portugueses de cassiterite e volframite. *Com. Serv. Geol. de Portugal*, 25, 251 pp.

Farias Arquer, P. (1992) El Paleozoico Inferior de la Zona de Galicia-Tras-os-Montes (Cordillera Herciniana, NW de España). In: "Paleozoico Inferior de Ibero-America", J.G. Gutiérrez Marco, J. Saavedra and Rábano I, eds. 495-504.

Freire D´Andrade, C. (1920) Contibutions for the study of the economic geology of Portugal. *Mem. Soc. Portug. Sc. Nat.* **1**, 1-32

Galliski, M. A., Černý, P., Márquez-Zavalia, M. F. and Chapman, R. (1999) Ferrotitanowodginite, $Fe^{2+}TiTa_2O_8$, a new mineral of the wodginite group from the San Elias pegmatite, San Luis, Argentina. *Amer. Mineral.* **84**: 773-777.

Gaspar, O., Bowles, J. F. W. and Shepherd, T. J. (1987) Silver mineralization at the Vale das Gatas tungsten mine, Portugal. *Min. Mag.* **51**, 305-310.

Gomes, M. E. P. (1996) Mineralogia, Petrologia e Geoquímica das rochas granitóides da área de Rebordelo-Bouça-Torre de D. Chama-Agrochão e as mineralizações associadas. Unpublished Ph. D. Thesis University of Trás-os-Montes e Alto Douro, Portugal, 323 pp.

Gomes, M. E. P. and A. M. R. Neiva (2002) Petrogenesis of tin-bearing granites from Ervedosa, northern Portugal: the importance of magmatic processes. *Chem. Erde* (in press).

Johan, V. and Johan, Z. (1994) Accessory minerals of the Cínovec (Zinnwald) granite cupola, Czech Republic. 1. Nb-, Ta- and Ti-bearing oxides. *Mineral. Petrol.* **51**, 323-343.

Kretschmar, U. & Scott, S. D. (1976) - Phase relations involving arsenopyrite in the system Fe-As-S and their application. *Can. Mineral.*, 14, 364-386.

Lécolle, M., Derré, C., Noronha, F. and Roger, G. 1981. Distribution des concentrations Sn-W dans le Nord du Trás-os-Montes (Portugal); typologies gîtologiques et mineralógiques. *In: Rappot final-ATP du CNRS* "Formation et distribution des gisements-1978", décision d´aide nº 3548, 19 pp.

Lehmann, B. (1990) Metallogeny of tin. Lecture notes in earth sciences, 32. Berlin: Springer-Verlag, 211pp.

Murciego, A., Garcia Sanchez, A., Dusausoy, Y., Martin Pozas, J.M. and Ruck, R.

(1997) - Geochemistry and EPR of cassiterites from Iberian Hercynian Massif. *Min. Mag.* **61**, 357-365.

Neiva, A. M. R. (1975) Geochemistry of coexisting aplites and pegmatites and their minerals from central northern Portugal. *Chem. Geology* **16**, 153-177.

Neiva, A. M. R. (1982) Geochemistry of muscovite and some physico-chemical conditions of some tin-tungsten deposits from Portugal. In: "Metallization associated with acid magmatism", A. M. Evans, ed., Vol. 6, Wiley, New York, 243-259.

Neiva, A. M. R. (1984) Geochemistry of tin-bearing granitic rocks. *Chem. Geology*, **43**, 241-256.

Neiva, A. M. R. (1987) Geochemistry of white micas from Portuguese tin and tungsten deposits. *Chem. Geology*, **63**, 299-317.

Neiva, A. M. R. (1993) Geochemistry of granites and their minerals from Gerez mountain, northern Portugal. *Chem. Erde.* **53**, 227-258.

Neiva, A. M. R. (1996) Geochemistry of cassiterite and its inclusions and exsolution products from tin and tungsten deposits in Portugal. *Can. Mineral.* **34**, 745-768.

Noronha, F.; Dória, M. A. and Pinto, M. S. (1987) The Murçós granitoid, an early granodiorite from NE Portugal associated with W-mineralization. *Abstract on Symposium*- The origin of granites, Edinburg.

Polya, D. A. (1988) Compositional variation in wolframites from the Barroca Grande mina, Portugal: evidence for fault-controlled ore formation. *Min. Mag.* **52**, 497-503.

Ribeiro, A. (1974) Contribuition l'étude tectonique de Trás-os-Montes Oriental. *Memórias Serviços Geológicos de Portugal* **24**, 168pp.

Ribeiro, A., Quesada, C. and Dallmeyer, R. D. (1990) Geodynamic evolution of the Iberian Massif. In: Dallmeyer, R. D., & Martinez Garcia, E. (eds) *Pré-Mesozoic Geology of Iberia,* Berlin: Springer-Verlag, 399-409.

Tindle, A.G., Breaks, F. W. and Webb, P. C. (1998) Wodginite-group minerals from the Separation Rapids rare-element granitic pegmatite group, northwestern Ontario. *Can. Mineral.* **34**, 745-768.

Uher, P., Cerny, P., Chapman, R., Határ, J. and Mike, O. (1998) Evolution of Nb, Ta-oxide minerals in the Prasiva granitic pegmatites, Slovakia. I. Primary Fe, Ti-rich assemblage, *Can. Mineral.* **36**, 525-534.

Recibido: Julio 2001
Aceptado: Diciembre 2001